# ULTIMATE STRENGTH AND INTERACTION CURVE OF STIFFENED PLATES SUBJECTED TO BIAXIAL IN-PLANE FORCES

Toshiyuki KITADA*, Hiroshi NAKAI**
and Tomiyasu FURUTA***

This paper deals with the ultimate strength of unstiffened and longitudinally stiffened plates subjected to biaxial in-plane forces. Firstly, the elastic buckling strength and corresponding buckling modes of stiffened plates are investigated in order to deduced the required minimum relative stiffness of a stiffener, and to decide the initial deflection modes of analytical models for analyzing the ultimate strength of stiffened plates parametrically. Then, the ultimate strength of unstiffened and stiffened plates are investigated through the elasto-plastic and finite displacement analyses on the basis of a finite element method. Finally, a simple and approximate interaction curve for the ultimate strength of unstiffened and stiffened plates is proposed.

**Keywords** : *unstiffened plate, stiffened plate, biaxial in-plane forces, ultimate strength, interaction curve, elastic buckling strength*

## 1. INTRODUCTION

In designing modern steel bridges, which are often constructed recently, the buckling stability of their lower flange and deck plates must be checked carefully as a stiffened plate subjected to biaxial in-plane forces. For example, these bridges are categorized as follows :

(1) Box girder bridges consisting of wide steel decks as the upper flange plates and slender floor beams, where the deck plates are subjected to not only the longitudinal in-plane stress due to the longitudinal bending but also the significant transverse in-plane stress due to the transverse bending.

(2) Cable-stayed bridges consisting of the wide and shallow main box girder, in which the steel deck plates and lower flange plates always undergo the longitudinal and transverse in-plane stresses.

(3) Arch bridges consisting of wide steel decks as the tie members and slender floor beams, where the longitudinal tension and the significant transverse compression occur simultaneously in the deck plates.

However, the current Japanese Specifications for Highway Bridges[1] (hereafter referred to as JSHB) does not codify any design criteria for the stiffened plates under biaxial in-plane stresses. Thus, the buckling stability must be investigated through theoretical and experimental studies, for checking

the safety of these flange and deck plates at the ultimate limit state in the case where the transverse compression due to the transverse bending is remarkably dominant. It is, therefore, preferable to establish a rational design method for such stiffened plates immediately. At present, the design methods for the stiffened plates subjected to the biaxial in-plane stresses are codified in BS 5400 Part 3[2], DIN 18800 Teil 3[3] and DDR-Standard[4].

In 1891, the first solution of the elastic linear buckling equation for an unstiffened plate under biaxial compressions was analyzed by Bryan[5]. Thereafter many studies have been conducted on the ultimate strength of unstiffened plate as listed in Table 1[6]-[17], and the interaction curves for the ultimate strength have been proposed by Lindner-Harbermann[7], Dier-Dowling[13] and Smith-Davidson-Chapman-Dowling[17]. However, there are only a few researches[18]-[20] on the ultimate strength of stiffened plates subjected to biaxial in-plane stresses, and the interaction curve for the ultimate strength of such plates have not sufficiently been investigated up to now.

This paper deals with such kind of problem in the following manners which are an expansion of the study in Ref.19). Firstly, the elastic buckling strength and buckling modes of stiffened plates are investigated. Secondly, the ultimate strength of unstiffened and stiffened plates with and without initial imperfections such as residual stress and initial deflection is examined through the elasto-plastic and finite displacement analysis. Finally, an interaction curve for predicting the ultimate strength of unstiffened and stiffened plates under biaxial in-plane stresses is proposed for the sake of design use.

* Member of JSCE, Dr. Eng., Associate Professor, Dept. of Civil Eng., Osaka City Univ. (Sugimoto 3-3-138, Sumiyoshi, Osaka 558)
** Member of JSCE, Dr. Eng., Professor, Dept. of Civil Eng., Osaka City Univ.
*** Member of JSCE, Dept. of Long Span Bridges, Yokogawa Construction Co. Ltd.

**Table 1** Previous works on biaxially loaded plates

| Analytical method / Model | Elastic buckling analysis | Elastoplastic buckling analysis | Elastic and finite displacement analysis | Elastoplastic and finite displacement analysis |
|---|---|---|---|---|
| Unstiffened plate | Bryan [5] (1891)<br>Ueda et al. [6] (1985)<br>Lindner -Habermann [7] (1988) | Inoue et al. [8] (1987) | Williams-Aalami [9] (1977)<br>Narayanan -Shanmugam [10] (1984)<br>Shen [11] (1989) | Valsgard [12] (1979)<br>Dier-Dowling [13] (1983)<br>Harding [14] (1983)<br>Ohtubo-Yoshida [15] (1984)<br>Taido et al. [16] (1985)<br>Smith et al. [17] (1987) |
| Stiffened plate | —— | —— | Ueda et al. [18] (1984) | Kitada et al. [19] (1988)<br>Dinkler-Kroplin [20] (1989) |
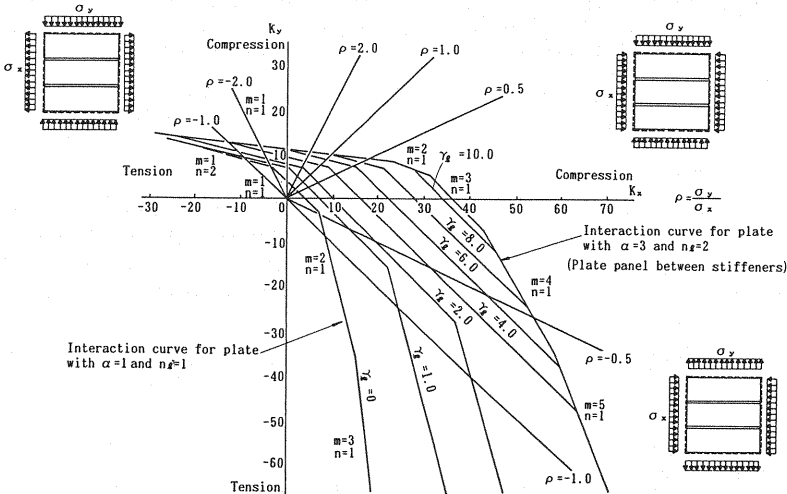


**Fig.2** Interaction curves of buckling coefficients between $k_x$ and $k_y$ for stiffend plate ($\alpha=1$, $\delta_1=0$ and 2-longitudinal stiffeners)
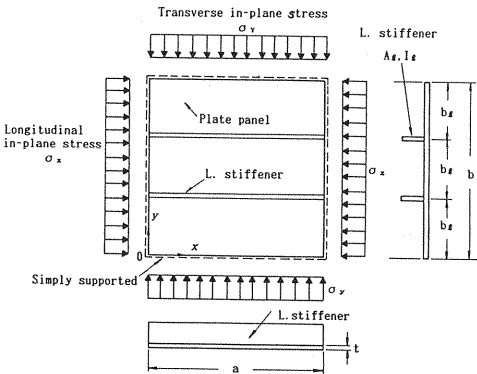


**Fig.1** Stiffened plate subjected to biaxially in-plane stresses $\sigma_x$ and $\sigma_y$

## 2. ELASTIC BUCKLING STRENGTH

### (1) Elastic buckling coefficient

A longitudinally stiffened plate with all the edges simply supported, shown in **Fig.1**, can be analyzed by using the sinusoidal buckling mode $w$ given by :

$$w = w_{mn} \sin\frac{m\pi x}{a} \sin\frac{n\pi y}{b} \quad\cdots\cdots\cdots\cdots\cdots ( 1 )$$

Therefore, the following elastic buckling stresses $\sigma_{xcr}$ and $\sigma_{ycr}$ will be obtained according to the energy method[21]:

$$\sigma_{xcr} = k_x \frac{E\pi^2}{12(1-\mu^2)}\left(\frac{t}{b}\right)^2,$$

$$\sigma_{ycr} = k_y \frac{E\pi^2}{12(1-\mu^2)}\left(\frac{t}{b}\right)^2, \quad k_y = \rho \cdot k_x$$

$$\cdots\cdots\cdots\cdots\cdots\cdots\cdots\cdots ( 2 )\sim( 4 )$$

where

$E$ : Young's modulus of steel

$\mu$ : Poisson's ratio of steel

and $k_x$ and $k_y$ are the elastic buckling coefficients expressed by the following equations :

$$k_x = \frac{\{(m/\alpha + \alpha n^2/m)^2 + (m/\alpha)^2(n_l+1)\gamma_l\}}{1 + \delta_l(n_l+1) + \rho(n\alpha/m)^2}$$

$$\cdots\cdots\cdots\cdots\cdots\cdots\cdots\cdots ( 5 )$$

$$k_y = (1/n\alpha^2 + n)^2 + (1/n^2\alpha^4)(n_l+1)\gamma_l,$$
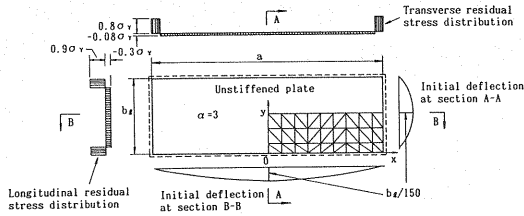
$$\text{(In the case of } \sigma_x=0) \cdots\cdots\cdots\cdots ( 6 )$$

**Fig.3** Model for unstiffened plate and assumed initial imperfections



(a) m=1, n=1      (b) m=2, n=1      (c) m=3, n=1
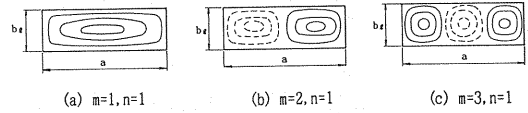
**Fig.4** Buckling modes of unstiffened plate ($\alpha=3$)

**Table 2** Range of parameters for unstiffened plate model



| $\alpha$ | $b_1/t$ | Imperfections | Material properties | Stress ratio $\rho$ |
|---|---|---|---|---|
| 3 | 20 | With I.D. and R.S. | $E= 2.1\times10^6$ kgf/cm$^2$ | |
| | 30 | With R.S. | $\sigma_Y= 2,400$ kgf/cm$^2$ | |
| | 40 | With I.D. | $\nu= 0.3$ | |
| | 60 | With Small I.I. | Perfect elasto-plastic | |

Where,
  I.D.: Initial deflection($b_1/150$, $\sigma_{rc}=0$)
  R.S.: Residual stress($\sigma_{rc}=-0.3\sigma_Y$, $b_1/1,500$)
  Small I.I.: Small initial imperfections
      ($b_1/1,500$, $\sigma_{rc}=0$)
  * :Longitudinal compression and transverse
      tension        (1kgf/cm$^2$=0.098MPa)

and
  $m$ : Number of half-waves of buckling mode in the direction of x-axis
  $n$ : Number of half-waves of buckling mode in the direction of y-axis
  $\alpha$ : Aspect ratio ($=a/b$)
  $\rho$ : Stress ratio ($=\sigma_y/\sigma_x$)
  $n_l$ : Number of longitudinal stiffeners
  $\gamma_l$ : Relative stiffness of a lngitudinal stiffener to plate ($=EI_l/bD$)
  $\delta_l$ : Area ratio of a longitudinal stiffener to plate ($=A_l/bt$)
  $A_l$ : Cross-sectional area of a longitudinal stiffener
  $I_l$ : Geometric moment of inertia of a longitudinal stiffener

## (2) Interaction curves of elastic buckling coefficients

As an illustrative example, $k_x$ and $k_y$ of a stiffened plate with $\alpha=1$ and $n_l=2$ are plotted in **Fig.2** by assuming the area ratio $\delta_l=0$ in Eq.(5). The required minimum relative stiffness of the stiffener $\gamma_l{}^*$ can generally be defined by the condition in which the elastic buckling stress of the overall stiffened plate is equal to that of the plate panel between the stiffeners[21]. It can be found in this example that $\gamma_l{}^*$ has a maximum value in the case where the stiffened plate is predominantly subjected to the longitudinal in-plane compression $\sigma_x$. These analytical results indicate that $\gamma_l{}^*$ is significantly sensitive to the stress ratio $\rho$, aspect ratio $\alpha$ and number of stiffeners $n_l$.

## 3. ULTIMATE STRENGTH AND INTERACTION CURVE

### (1) Unstiffened plate

**a) Model and initial imperfections**

The model, shown in **Fig.3**, is adopted in the numerical calculations for unstiffened plates. This figure also illustrates the initial deflection and residual stress considered in this model.

The biaxial in-plane stresses $\sigma_x$ and $\sigma_y$ are introduced by specifying longitudinal and transverse in-plane displacements which are distributed uniformly along the transverse and longitudinal edges respectively, because of the function of the computer program[22] used for the numerical calculations.

The ratio of the longitudinal and transverse displacements along the edges is determined so that an expected stress ratio $\rho$ can be evaluated by the model assumed to be of elastic and linear body. Therefore, the displacement ratio is kept constant in all the stages of analysis, but the ratio of the longitudinal and transverse average stresses $\sigma_x$ and $\sigma_y$ is not kept constant up to the ultimate state.

The predominate elastic buckling mode of an unstiffened plate with $\alpha=3$ varies among the modes illustrated in **Fig.4** as the combination of longitudinal and transverse stresses varies. Accordingly, the elasto-plastic and finite displacement analysis[22] is carried out for the plates with three types of the initial deflection similar to three buckling modes, shown in **Fig.4**, in order to obtain the smallest ultimate strength.
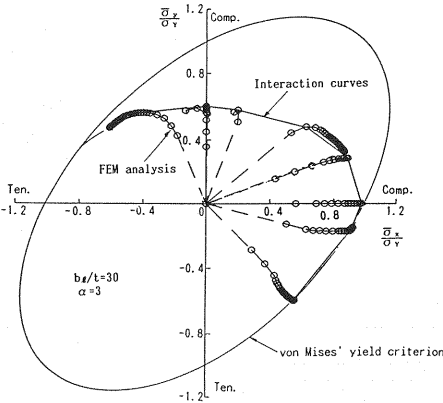
**Fig.5** Stress paths and interaction curve for unstiffened plate ($\alpha=3$ and $b_l/t=30$)



**Fig.6** Approximate interaction curve for ultimate strength of unstiffened plate

**Table.2** summarizes the range of parameters used for investigating the ultimate strength of unstiffened plates.

**b)** Ultimate strength and interaction curves

**Fig.5** shows the stress paths of the unstiffened plates with $\alpha=3$ and $b_l/t=30$, an interaction curve which envelops the ultimate states of the paths (hereafter called as the interaction curve for ultimate strength), and the yield criteria of von Mises. One of the mean axial stress components $\sigma_x$ and $\sigma_y$ attains its maximum value $\sigma_{xm}$ or $\sigma_{ym}$ and then decreases, while another component increases monotonically. However, a point where one of the mean axial stress components attains to the maximum value should be defined as the ultimate state of the plate from the point of design use.

**c)** Approximate interaction curves for ultimate strength

**Fig.6** replots the numerical results of **Fig.5** by using the ordinate $\sigma_{ym}/\sigma_{ymo}$ and the abscissa $\sigma_{xm}/\sigma_{xmo}$, where $\sigma_{xmo}$ and $\sigma_{ymo}$ are the longitudinal and transverse ultimate stresses of unstiffened plate subjected to the longitudinal and transverse compressions alone respectively. It is found from the numerical results as shown in this figure as one example that the ultimate state can be approximated adequately by a simple interaction curve decided on the basis of trial and error method, which is defined as follows :

1) In the case of plates under biaxial in-plane tensions

The ultimate strength of unstiffened plate is defined by the von Mises yield criterion given by :

$$\left(\frac{\sigma_{xm}}{\sigma_Y}\right)^2-\frac{\sigma_{xm}}{\sigma_Y}\frac{\sigma_{ym}}{\sigma_Y}+\left(\frac{\sigma_{ym}}{\sigma_Y}\right)^2=1 \cdots\cdots\cdots (7)$$

2) In the case of plates under longitudinal tension and transverse compression
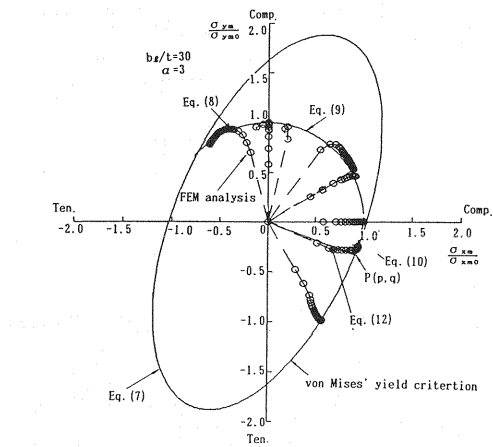
The ultimate state is defined by :

$$\left(\frac{\sigma_{xm}}{\sigma_Y}\right)^2+\left(\frac{\sigma_{ym}}{\sigma_{ymo}}\right)^2=1 \cdots\cdots\cdots\cdots (8)$$

However, Eq.(7) should be used where the locus of Eq.(8) is located outside that of Eq.(7).

3) In the case of plates under biaxial compressions

The ultimate state is expressed by :

$$\left(\frac{\sigma_{xm}}{\sigma_{xmo}}\right)^2+\left(\frac{\sigma_{ym}}{\sigma_{ymo}}\right)^2=1 \cdots\cdots\cdots\cdots (9)$$

4) In the case of plates under longitudinal compression and transverse tension

The following equation defines the ultimate state :

$$\frac{\sigma_{ym}}{\sigma_{ymo}}=\frac{q}{p-1}\left(\frac{\sigma_{xm}}{\sigma_{xmo}}-1\right) \cdots\cdots\cdots (10)$$

where

$$p=$$

$$\cfrac{1}{\left(\dfrac{\sigma_{xmo}}{\sigma_Y}\right)\sqrt{1+\left(\left(\dfrac{\sigma_{ymo}}{\sigma_Y}\right)\cos^{-1}\left(\dfrac{\sigma_{xmo}}{\sigma_Y}\right)\right)^2}+\left(\dfrac{\sigma_{ymo}}{\sigma_Y}\right)\cos^{-1}\left(\dfrac{\sigma_{xmo}}{\sigma_Y}\right)}$$

$$\cdots\cdots\cdots\cdots (11)$$

$$q=-p\left(\frac{\sigma_{xmo}}{\sigma_Y}\right)\cos^{-1}\left(\frac{\sigma_{xmo}}{\sigma_Y}\right) \cdots\cdots\cdots (12)$$

However, Eq.(7) should be used where the locus of Eq.(10) is located outside that of Eq.(7).

**d)** Effect of width-thickness ratio on interaction curves for ultimate strength

The effect of the width-thickness ratio $b_l/t$ on the interaction curve for ultimate strength is illustrated in **Fig.7**. It can be seen that the interaction curves for ultimate strength reach the von Mises yield criterion as $b_l/t$ decreases.

**e)** Effect of initial imperfections

**Fig.8** shows the approximate interaction curves for ultimate strength of plates having various combinations of initial imperfections. The effect of
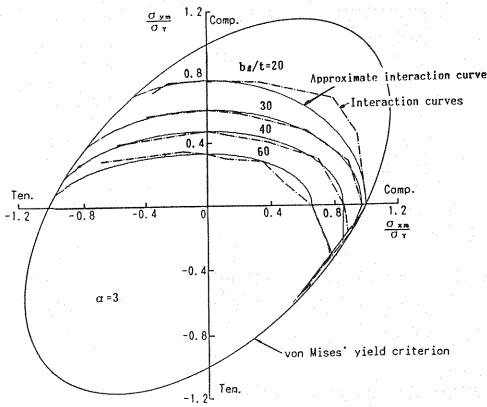
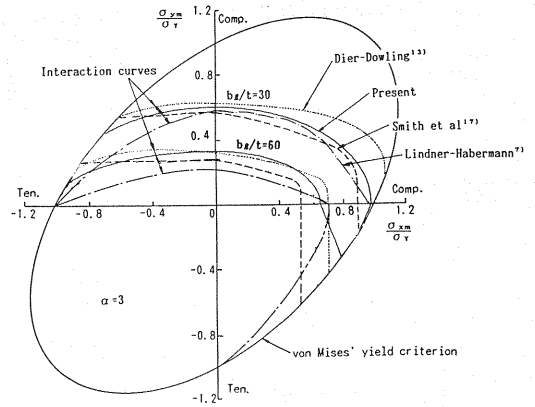**Fig.7** Variation of interaction curves for ultimate strength of unstiffened plate due to width-thickness ratio



**Fig.9** Comparison of approximate interaction curves for ultimate strength of unstiffened plate
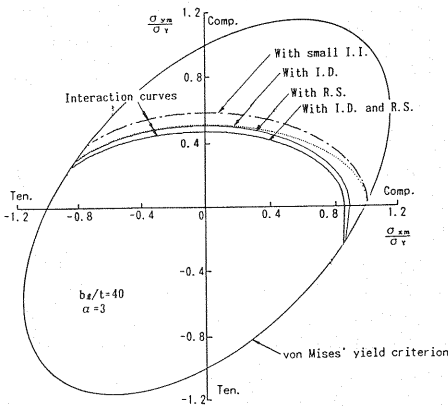


**Fig.8** Variation of approximate interaction curves for ultimate strength of unstiffened plate due to initial imperfections
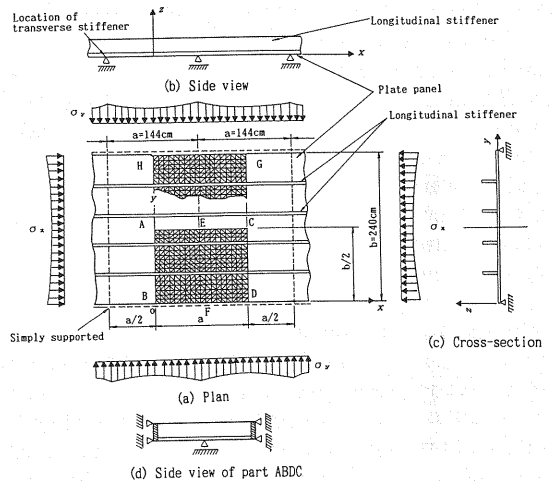


**Fig.10** Example of model for stiffened plate with 4-longitudinal stiffeners

initial deflections and residual stresses on the ultimate strength can not be neglected under any combinations of applied biaxial in-plane stresses.

**f) Comparison of interaction curves**

In **Fig.9**, the approximate interaction curves for ultimate strength of the unstiffened plates with $\alpha = 3$ and $b_t/t = 30$ and 60 are compared with the interaction curves proposed by Lindner-Harbermann[7], Dier-Dowling[13] and Smith et al.[17]. These interaction curves seem to have almost the same trend in the shape, although the boundary conditions and initial imperfections under consideration are slightly different from each other. The proposed curves are located almost in the center of these curves.

**(2) Stiffened Plate**

**a) Model for stiffened plate and initial imperfections**

An infinitely long model, shown in **Fig.10**, is adopted in the numerical calculations to investigate the ultimate strength of stiffened plate. The longitudinal edges of this model are assumed to be simply supported. The deflections are restricted at the transverse supports which correspond to the locations of transverse stiffeners. Only the part ABDC or HBDG in this figure is analyzed in numerical calculations by the use of the symmetry of the model structure as well as the symmetric and anti-symmetric patterns of deflection and initial deflection.

As a typical example, **Fig.11** illustrates the initial deflection and residual stress distributions adopted in an model with two stiffeners.

The initial deflection of stiffened plate model is given as the summation of the global initial deflection mode for the overall stiffened plate model and the local initial deflection mode of plate panels between stiffeners. For instance, **Fig.12**
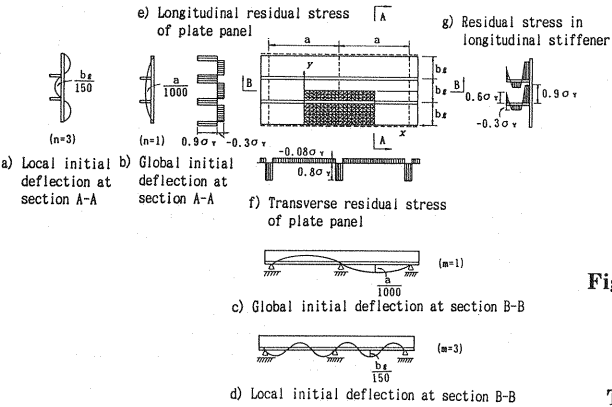
**Fig.11** Example of initial deflection and residual stress distributions in stiffened plate model with 2-longitudinal stiffeners



**Fig.12** Global and local initial deflection modes for stiffened plate model with 2-longitudinal stiffeners

**Table 3** Range of parameters for stiffened plate model

| $n_l$ | $\gamma_l^*$ | $\alpha$ | $b_l/t$ | Imperfections | Material properties | $\rho$ |
|---|---|---|---|---|---|---|
| 2 | 0.5 | 1 | 20 | With I.D. and R.S. | $E= 2.1\times10^6$ kgf/cm² | -1.0 |
| 4 | 1.0 | 0.6 | 30 | With R.S. | $\sigma_Y= 2,400$ kgf/cm² | -4.0 |
|  | 2.0 |  | 40 | With I.D. | $\nu= 0.3$ | ∞ |
|  |  |  | 60 | With Small I.I. | Perfect elasto-plastic | 4.0 |

Where,
(1kgf/cm²=0.098MPa)   1.0
I.D.: Initial deflection (a/1,000, $b_l/150$ $\sigma_{rc}$=0)   0.25
R.S.: Residual stress($\sigma_{rc}$=-0.3$\sigma_Y$ and (a/10,000, $b_l/1,500$))   0.0
Small I.I.: Small initial imperfections(a/10,000,$b_l/1,500$   -0.25*
and $\sigma_{rc}$=0),   $\rho$ : Stress ratio   -1.0*
$n_l$ : Number of stiffeners,   $\gamma_l^*$: Relative stiffness
*:Longitudinal compression and transverse tension

shows the global and local initial deflection modes which are used in the numerical calculations for a stiffened plate model with 2-stiffeners. A few combinations of these global and local initial deflection modes, which are similar to the elastic buckling modes, are used in order to obtain the smallest ultimate strength of one stiffened plate model under one combinations of longitudinal and transverse stresses. The model of the part HBDG is adopted in the case where the stiffened plate models have the anti-symmetrical initial deflection modes in the transverse direction. The initial deflection modes are sinusoidal in both the longitudinal and transverse directions. The magnitudes of the initial deflection modes are taken as $a/1,000$ for the global one, and $b_l/150$ for the local one according to JSHB.

The longitudinal and transverse residual stress distributions, which satisfy the conditions of self-equilibrium with respect to in-plane force and out-of-plane bending moment, are applied to the models. The longitudinal residual stress distribution is chosen according to Ref.23) which proposes the actual distribution.

**Table 3** summarizes the range of parameters to investigate the variations of the ultimate strength of stiffened plate. The ratio of the height $h_r$ to thickness $t_r$ of stiffener is kept constant ($h_r/t_r=$ 13), because the local buckling of stiffener is not considered in the calculation. The relative stiffness of stiffeners $\gamma_l^*$ is decided using Eqs.(2)-(6).

**b)** Behaviors up to ultimate state

In order to examine the behavior of a stiffened plate subjected to the biaxial in-plane stresses up to the ultimate state, shown in **Fig.13** are the relationships between the applied longitudinal mean stress $\bar{\sigma}_x/\sigma_Y$ and longitudinal local stress $\bar{\sigma}_x/\sigma_Y$ in the representative points of the stiffened
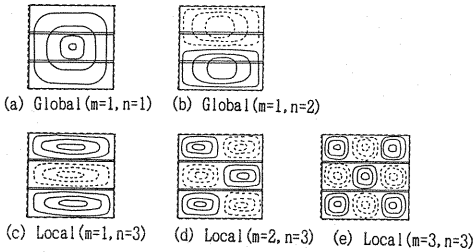
plate model with two longitudinal stiffeners ($b_l/t=$ 40, $\gamma_l=\gamma_l^*$, and $\rho=1.0$).

**Figs.13** (b) and (c) correspond to the numerical results of the stiffened plate without residual stress, and **Figs.13** (d) and (e) are for the stiffened plate with residual stress. It can be seen from the difference of the stresses at both the surfaces of plate panel or the stresses at the bottom and top of stiffener that the in-plane bending moment of the stiffener and out-of-plane bending moment of the plate panel increase gradually. Consequently, the stiffened plates reach the ultimate state, because of the decrease of stiffness due to the partial yielding of the plate panels at the section A-A and the partial yielding of the plate panel and stiffeners at the section B-B.

**c)** Ultimate strength

The numerical results are plotted in **Fig.14** for the stiffened plate models with $b_l/t=30$ and $\gamma_l=$ $\gamma_l^*$. Ordinate and abscissa of this figure are the transverse $\sigma_Y$ and longitudinal mean stresses $\sigma_x$ divided by the yield stress $\sigma_Y$ respectively. The stress paths obtained from the elasto-plastic and finite displacement analysis are plotted together with the von Mises yield criteria of both the plate panel and stiffened plate. The yield criterion of stiffened plate is derived by assuming that the plate panel conforms to von Mises criterion, whereas the longitudinal stiffeners are subjected to longitudinal stress alone. However, the yield criterion of von Mises can be adopted for stiffened plate, because these two yield criteria are almost the same. It can
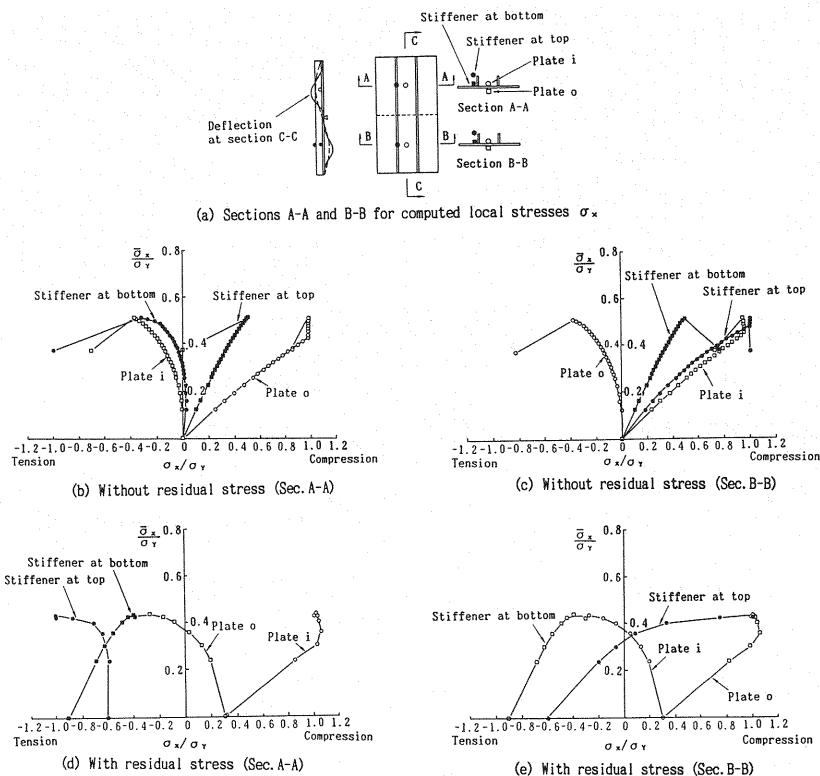
(a) Sections A-A and B-B for computed local stresses $\sigma_x$

(b) Without residual stress (Sec. A-A)

(c) Without residual stress (Sec. B-B)

(d) With residual stress (Sec. A-A)

(e) With residual stress (Sec. B-B)

**Fig. 13** Relationships between longitudinal mean compressive stress $\bar{\sigma}_x$ and local stress $\bar{\sigma}_x$ ($b_l/t=40$, $\gamma_l=\gamma_l{}^*$, $\rho=1.0$ and 2-longitudinal stiffeners)
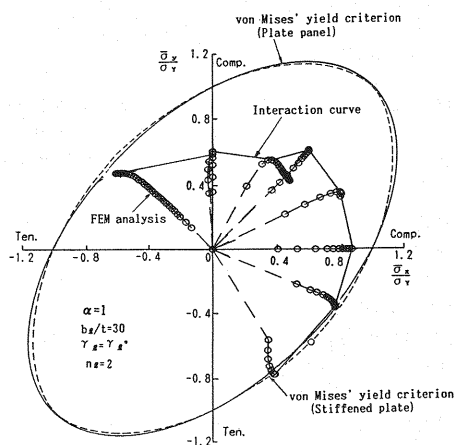


**Fig. 14** Stress paths and interaction curve for ultimate strength of stiffened plate model ($b_l/t=30$, $\gamma_l=\gamma_l{}^*$, $\rho=1.0$ and 2-longitudinal stiffeners)
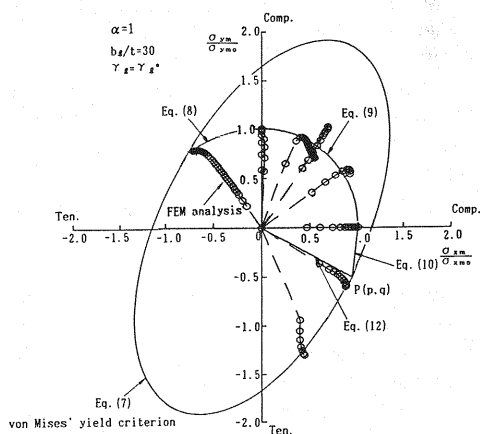


**Fig. 15** Approximate interaction curve for ultimate strength of stiffened plate

be seen from this figure that the ultimate states of stress paths can fairly be enveloped by an interaction curve.

The similar results are also obtained for the stiffened plate models with four longitudinal stiffeners.

**d) Approximate interaction curves for ultimate strength**

**Fig. 15** replots the numerical results in **Fig. 14** with abscissa $\sigma_{xm}/\sigma_{xmo}$ and ordinate $\sigma_{ym}/\sigma_{ymo}$. The ultimate state of the stiffened plate subjected to biaxial in-plane stresses can also be expressed accurately by the same approximate interaction
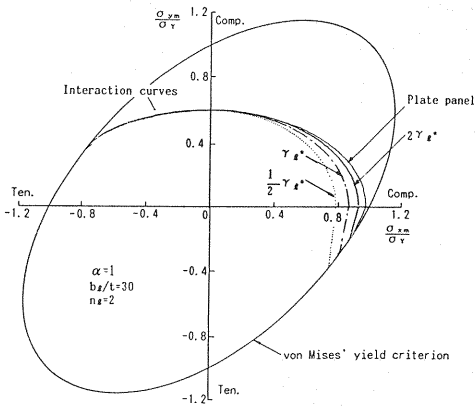
**Fig.16** Variations of approximate interaction curves for ultimate strength due to relative stiffness ($b_l/t=30$, 2-longitudinal stiffeners)
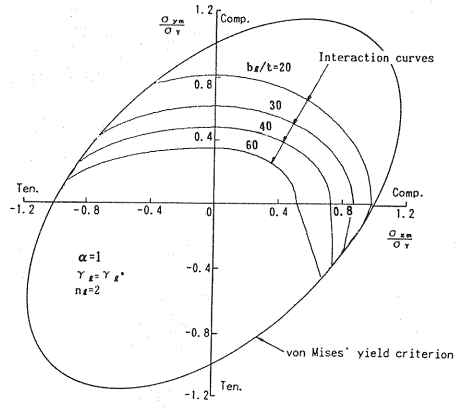


**Fig.18** Variations of approximate interaction curves for ultimate strength of stiffened plates due to width-thickness ratio ($\gamma_l=\gamma_l{}^*$, 2-longitudinal stiffeners)
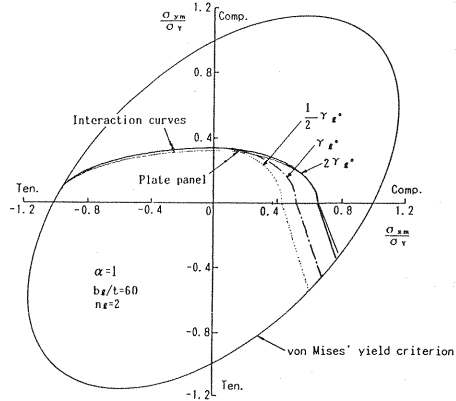


**Fig.17** Variations of approximate interaction curves for ultimate strength due to relative stiffness ($b_l/t=60$, 2-longitudinal stiffeners)
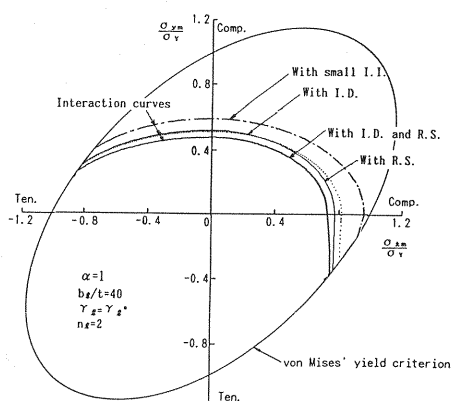


**Fig.19** Variations of approximate interaction curves for ultimate strength of stiffened plates with initial imperfections ($\gamma_l=\gamma_l{}^*$, 2-longitudinal stiffeners)

curve as that for the unstiffened plate, which is expressed in Eq.(7) through Eq.(12), if the longitudinal and transverse ultimate stresses of the stiffened plate instead of the unstiffened plate are taken as $\sigma_{xmo}$ and $\sigma_{ymo}$.

**e)** Effect of relative stiffness on approximate interaction curves for ultimate strength

**Figs.16** and **17** show the variations of the approximate interaction curves for ultimate strength of the stiffened plate models with various relative stiffness of longitudinal stiffener to the plate panel $\gamma_l$ compared with that of the plate panel between stiffeners. The approximate interaction curves for ultimate strength of stiffened plates approach that of the plate panel in accordance with the increase of $\gamma_l$. The difference of the transverse ultimate strengths between the plate panel and stiffened plates is caused by the deviation of the initial deflection modes adopted in the numerical

analysis. From the conservative point of view, the transverse ultimate strength of the plate panel alone can be used as that of the stiffened plate.

It should be noted from these two figures that the transverse ultimate stress in the region of small longitudinal stress does not depend on the relative stiffness $\gamma_l$, while the longitudinal ultimate stress in the region of small transverse stress increases in accordance with the increase of the relative stiffness. This tendency becomes remarkable with the increase of the width-thickness ratio.

**f)** Effect of width-thickness ratio on approximate interaction curves for ultimate strength

The effect of width-thickness ratio $b_l/t$ on the approximate interaction curve for ultimate strength is illustrated in **Fig.18**. The approximate interaction curves for ultimate strength reach the von Mises yield criterion as $b_l/t$ decreases.

**g)** Effect of initial imperfections on approxi-

mate interaction curves for ultimate strength

**Fig.19** shows the approximate interaction curves for ultimate strength with different magnitudes of the initial imperfections. It can be seen that the effect of initial deflections and residual stresses on the ultimate strength can not be neglected under any combinations of applied biaxial in-plane stresses.

## 4. PROPOSITION OF APPROXIMATE METHOD FOR PREDICTING ULTIMATE STRENGTH

A simple and approximate interaction curve for ultimate strength, which is expressed by the function of the longitudinal ultimate stress $\sigma_{xmo}$ and transverse ultimate stress $\sigma_{ymo}$, is proposed in the previous sections for predicting the ultimate strengths $\sigma_{xm}$ and $\sigma_{ym}$ of unstiffened and stiffened plates subjected to biaxial in-plane stresses.

In deducing this approximate interaction curve for ultimate strength, the actual transverse residual stress distribution based on the measured data is not used in this study. However, the ultimate strength of ordinary stiffened plates under biaxial in-plane stresses can be predicted by this approximate interaction curve for ultimate strength proposed in this paper, if the transverse ultimate stress $\sigma_{ymo}$, which is derived based on the actual residual distribution, is used. Because it is considered that the shape of the approximate interaction curve for ultimate strength does not vary significantly, even if the pattern of the transverse residual stress is like the actual one.

Incidentally, the approximate longitudinal ultimate stresses of unstiffened and stiffened plates can be obtained, for instance, by using the ultimate strength curves in Ref.22) and the column approach proposed in Ref.24), respectively. It is, however, necessary to develop a simple method for predicting the transverse ultimate stress of unstiffened and stiffened plates with the actual residual stress[19].

## 5. CONCLUSION

The main conclusions obtained by this paper are outlined as follows :

1) According to the elastic buckling theory, the elastic buckling coefficients of stiffened plate subjected to biaxial in-plane stresses have been derived by the energy method.

2) The required minimum relative stiffness of the stiffener of stiffened plates under biaxial in-plane forces varies significantly in accordance with the aspect ratio, number of stiffeners, and stress ratio.

3) Based on the elasto-plastic and finite displacement analysis, an approximate interaction curve for ultimate strength is proposed for predicting the ultimate strength of unstiffened and stiffened plates subjected to biaxial in-plane stresses, and can be expressed by the function of the longitudinal and transverse ultimate stresses.

4) The interaction curves for ultimate strength of unstiffened and stiffened plates have a tendency to approach the yield criteria of von Mises as the width thickness ratio becomes small.

5) The ultimate strength of the stiffened plate predominantly subjected to the longitudinal compression increases as the stiffness of stiffener increases, while the ultimate strength of stiffened plate dominantly subjected to the transverse compression does not increase in accordance with the increase of the stiffness of the stiffener.

6) The effect of initial deflections and residual stresses on the ultimate strength can not be neglected under any combinations of applied biaxial in-plane stresses.

### REFERENCES

1) Japanese Road Association : Japanese Specifications for Highway Bridges, Part II, Steel Bridges, Maruzen, Feb. 1990.

2) British Standards Institution : BS5400, Part 3, Code of practice for design of steel bridges, Apr. 1982.

3) DIN 18800 Teil 3, Stahlbauten Stabilitätsfälle-Plattenbeulen, Norm-Vorlage, Aug./Nov. 1986.

4) DDR-Standard, Stabilität von Stahltragwerken, Apr. 1982.

5) Brayan, G.H. : On the stability of a plane plate under thrust in its own plane with application to the buckling of the side of a ship, Proceedings of the London Mathematical Society, Vol.22, pp.54~67, Nov. 1891.

6) Ueda, Y., Rashed, S.M.H. and Paik, J.K. : Elastic buckling interaction equation of simply supported rectangular plates subjected to five loaded components, Journal of the Society of Naval Architects of Japan, No.157, pp.425~438, Jun 1985.

7) Lindner, J. and Habermann, W. : Zur Weierentwicklung des Beulnachweises für Platten bei mehrachsiger Beanspruchung, Der Stahlbau, 57.Jahrgang, S.333~339, Heft 11, Nov. 1988.

8) Inoue, T., Komiya, N. and Kato, B. : Flexural rigidities and buckling of steel plates in the plastic flow range under

biaxial stress, Architectural Institute of Japan, No.371, pp.1~13, Jan. 1987.

9) Williams, D.G. and Aalami, B. : Thin Plate Design for In-plane Loading, Granada, 1979.

10) Narayanan, R. and Shanmugam, N.E. : Compressive strength of biaxially loaded plates, Plated Structures - Stability and Strength, Edited by Narayanan, R., Elsevier, pp.195~221, 1983.

11) Shen, H. : Postbuckling behavior of rectangular plates under combined loading, Journal of Thin-Walled Structures, Vol.8, pp.203~216, 1989.

12) Valsgård, S. : Numerical design prediction of the capacity of plates in biaxial in-plane compression, Journal of Computer & Structures, Vol.12, pp.729~739, 1980.

13) Dier, A.F., and Dowling, P.J. : The strength of plates subjected to biaxial forces, Behavior of Thin-Walled Structures, Edited by Rhodes, J. and Spence, J., Elsevier, pp.329~353, 1984.

14) Harding, J.E. : The interaction of direct and shear stresses on plate panels, Plated Structures - Stability and Strength, Edited by Narayanan, R., Elsevier, pp.221~255, 1983.

15) Ohtsubo, H. and Yoshida, J. : Ultimate strength of rectangular plates under combination of loads, Part 1 - Biaxial compression, Journal of the Society of Naval Architects of Japan, No.157, pp.425~438, Jun 1985.

16) Taido, Y., Hayashi, H., Kitada, T. and Nakai, H. : A design method of wide stiffened plates subjected to uniaxial and biaxial compression, Der Stahlbau, 54 Jahrgang, Heft 5, S.149~155, May 1985.

17) Smith, C.S., Davidson, P.P., Chapman, J.C. and Dowling, P.J. : Strength and stiffness of ships' plating under in-plane compression and tension, The Royal Institute of Naval Architects, W6, pp.1~17, 1987.

18) Ueda, Y., Rashed, S.M.H. and Paik, J.K. : Buckling and ultimate strength interactions of plates and stiffened plates under combined loads, 1st Report, In-plane biaxial and shearing forces, Journal of the Society of Naval Architects of Japan, No.156, pp.355~365, Nov. 1984.

19) Kitada, T., Nakai, H., Furuta, T. and Suzuki, H. : Ultimate strength of stiffened plates subjected to biaxial in-plane forces, Journal of Structural Engineering, JSCE, Vol.34A, pp.203~214, May 1988.

20) Dinkler, D. and Kröplin, B. : Biaxial stress interaction for local elasto-plastic buckling of stiffened plates, Proceedings of ECCS Colloquium on Stability of Plate and Shell Structures, Ghent University, pp.179~188, Apr. 1987.

21) Timoshenko, S.P. and Gere, J.M. : Theory of Elastic Stability, McGraw-Hill, 1961.

22) Komatsu, S. and Kitada, T. : A study on the ultimate strength of compression plate with initial imperfections, Proceedings of JSCE, No.270, pp.1~14, Feb. 1978.

23) Komatsu, S., Usio, M. and Kitada, T. : An experimental study on residual stresses and initial deformations of stiffened plates, Proceedings of JSCE, No.265, pp.25~35, Sept. 1977.

24) Nakai, H., Taido, Y. ,Kitada, T. and Hayashi, H. : A design method for othogonally stiffened plates with or without stringers subjected to uniaxial compression, Proceedings of JSCE, Structural Eng./Earthquake Eng., Vol.2, No.2, pp.301s~310s, Oct. 1985.